ALMA MATER STUDIORUM
UNIVERSITÀ DI BOLOGNA

ARCHIVIO ISTITUZIONALE
DELLA RICERCA

Alma Mater Studiorum Università di Bologna
Archivio istituzionale della ricerca

Joint Constraints on Galactic Diffuse Neutrino Emission from the ANTARES and IceCube Neutrino Telescopes

This is the final peer-reviewed author's accepted manuscript (postprint) of the following publication:

Published Version:
Albert, A., André, M., Anghinolfi, M., Ardid, M., Aubert, J., Aublin, J., et al. (2018). Joint Constraints on Galactic Diffuse Neutrino Emission from the ANTARES and IceCube Neutrino Telescopes. THE ASTROPHYSICAL JOURNAL LETTERS, 868(2), 1-9 [10.3847/2041-8213/aaeecf].

Availability:
This version is available at: https://hdl.handle.net/11585/658666 since: 2019-01-30

Published:
DOI: http://doi.org/10.3847/2041-8213/aaeecf

Terms of use:

Some rights reserved. The terms and conditions for the reuse of this version of the manuscript are specified in the publishing policy. For all terms of use and more information see the publisher's website.

This item was downloaded from IRIS Università di Bologna (https://cris.unibo.it/).
When citing, please refer to the published version.

(Article begins on next page)

12 October 2024

This is the final peer-reviewed accepted manuscript of:

A. Albert et al., *Joint Constraints on Galactic Diffuse Neutrino Emission from the ANTARES and IceCube Neutrino Telescopes*, 2018 ApJL 868 L20.

The final published version is available at: https://doi.org/10.3847/2041-8213/aaeecf

Rights / License:

The terms and conditions for the reuse of this version of the manuscript are specified in the publishing policy. For all terms of use and more information see the publisher's website.

This item was downloaded from IRIS Università di Bologna (https://cris.unibo.it/)

When citing, please refer to the published version.

Draft version November 15, 2018
Typeset using LaTeX **twocolumn** style in AASTeX62

Joint constraints on Galactic diffuse neutrino emission from the ANTARES and IceCube neutrino telescopes

ANTARES collaboration

A. Albert,[1] M. André,[2] M. Anghinolfi,[3] M. Ardid,[4] J.-J. Aubert,[5] J. Aublin,[6] T. Avgitas,[6] B. Baret,[6] J. Barrios-Martí,[7] S. Basa,[8] B. Belhorma,[9] V. Bertin,[5] S. Biagi,[10] R. Bormuth,[11,12] J. Boumaaza,[13] S. Bourret,[6] M.C. Bouwhuis,[11] H. Brânzaş,[14] R. Bruijn,[11,15] J. Brunner,[5] J. Busto,[5] A. Capone,[16,17] L. Caramete,[14] J. Carr,[5] S. Celli,[16,17,18] M. Chabab,[19] R. Cherkaoui El Moursli,[13] T. Chiarusi,[20] M. Circella,[21] J.A.B. Coelho,[6] A. Coleiro,[7,6] M. Colomer,[6,7] R. Coniglione,[10] H. Costantini,[5] P. Coyle,[5] A. Creusot,[6] A. F. Díaz,[22] A. Deschamps,[23] C. Distefano,[10] I. Di Palma,[16,17] A. Domi,[3,24] C. Donzaud,[6,25] D. Dornic,[5] D. Drouhin,[26] T. Eberl,[27] I. El Bojaddaini,[28] N. El Khayati,[13] D. Elsässer,[29] A. Enzenhöfer,[27,5] A. Ettahiri,[13] F. Fassi,[13] I. Felis,[4] P. Fermani,[16,17] G. Ferrara,[10] L. Fusco,[6,30] P. Gay,[31,6] H. Glotin,[32] T. Grégoire,[6] R. Gracia Ruiz,[26] K. Graf,[27] S. Hallmann,[27] H. van Haren,[33] A.J. Heijboer,[11] Y. Hello,[23] J.J. Hernández-Rey,[7] J. Hössl,[27] J. Hofestädt,[27] G. Illuminati,[7] C.W. James,[27] M. de Jong,[11,12] M. Jongen,[11] M. Kadler,[29] O. Kalekin,[27] U. Katz,[27] N.R. Khan-Chowdhury,[7] A. Kouchner,[6,34] M. Kreter,[29] I. Kreykenbohm,[35] V. Kulikovskiy,[3,36] C. Lachaud,[6] R. Lahmann,[27] D. Lefèvre,[37] E. Leonora,[38] G. Levi,[20,30] M. Lotze,[7] S. Loucatos,[39,6] M. Marcelin,[8] A. Margiotta,[20,30] A. Marinelli,[40,41] J.A. Martínez-Mora,[4] R. Mele,[42,43] K. Melis,[11,44] P. Migliozzi,[42] A. Moussa,[28] S. Navas,[45] E. Nezri,[8] A. Nuñez,[5,8] M. Organokov,[26] G.E. Păvălaş,[14] C. Pellegrino,[20,30] P. Piattelli,[10] V. Popa,[14] T. Pradier,[26] L. Quinn,[5] C. Racca,[46] N. Randazzo,[38] G. Riccobene,[10] A. Sánchez-Losa,[21] M. Saldaña,[4] I. Salvadori,[5] D. F. E. Samtleben,[11,12] M. Sanguineti,[3,24] P. Sapienza,[10] F. Schüssler,[39] M. Spurio,[20,30] Th. Stolarczyk,[39] M. Taiuti,[3,24] Y. Tayalati,[13] A. Trovato,[10] B. Vallage,[39,6] V. Van Elewyck,[6,34] F. Versari,[20,30] D. Vivolo,[42,43] J. Wilms,[35] D. Zaborov,[5] J.D. Zornoza,[7] and J. Zúñiga[7]

IceCube Collaboration

M. G. Aartsen,[47] M. Ackermann,[48] J. Adams,[49] J. A. Aguilar,[50] M. Ahlers,[51] M. Ahrens,[52] I. Al Samarai,[53] D. Altmann,[54] K. Andeen,[55] T. Anderson,[56] I. Ansseau,[50] G. Anton,[54] C. Argüelles,[57] J. Auffenberg,[58] S. Axani,[57] P. Backes,[58] H. Bagherpour,[49] X. Bai,[59] A. Barbano,[53] J. P. Barron,[60] S. W. Barwick,[61] V. Baum,[62] R. Bay,[63] J. J. Beatty,[64,65] J. Becker Tjus,[66] K.-H. Becker,[67] S. BenZvi,[68] D. Berley,[69] E. Bernardini,[48] D. Z. Besson,[70] G. Binder,[71,63] D. Bindig,[67] E. Blaufuss,[69] S. Blot,[48] C. Bohm,[52] M. Börner,[72] F. Bos,[66] S. Böser,[62] O. Botner,[73] E. Bourbeau,[51] J. Bourbeau,[74] F. Bradascio,[48] J. Braun,[74] M. Brenzke,[58] H.-P. Bretz,[48] S. Bron,[53] J. Brostean-Kaiser,[48] A. Burgman,[73] R. S. Busse,[74] T. Carver,[53] E. Cheung,[69] D. Chirkin,[74] A. Christov,[53] K. Clark,[75] L. Classen,[76] G. H. Collin,[57] J. M. Conrad,[57] P. Coppin,[77] P. Correa,[77] D. F. Cowen,[56,78] R. Cross,[68] P. Dave,[79] M. Day,[74] J. P. A. M. de André,[80] C. De Clercq,[77] J. J. DeLaunay,[56] H. Dembinski,[81] K. Deoskar,[52] S. De Ridder,[82] P. Desiati,[74] K. D. de Vries,[77] G. de Wasseige,[77] M. de With,[83] T. DeYoung,[80] J. C. Díaz-Vélez,[74] V. di Lorenzo,[62] H. Dujmovic,[84] J. P. Dumm,[52] M. Dunkman,[56] E. Dvorak,[59] B. Eberhardt,[62] T. Ehrhardt,[62] B. Eichmann,[66] P. Eller,[56] P. A. Evenson,[81] S. Fahey,[74] A. R. Fazely,[85] J. Felde,[69] K. Filimonov,[63] C. Finley,[52] A. Franckowiak,[48] E. Friedman,[69] A. Fritz,[62] T. K. Gaisser,[81] J. Gallagher,[86] E. Ganster,[58] L. Gerhardt,[71] K. Ghorbani,[74] W. Giang,[60] T. Glauch,[87] T. Glüsenkamp,[54] A. Goldschmidt,[71] J. G. Gonzalez,[81] D. Grant,[60] Z. Griffith,[74] C. Haack,[58] A. Hallgren,[73] L. Halve,[58] F. Halzen,[74] K. Hanson,[74] D. Hebecker,[83] D. Heereman,[50] K. Helbing,[67] R. Hellauer,[69] S. Hickford,[67] J. Hignight,[80] G. C. Hill,[88] K. D. Hoffman,[69] R. Hoffmann,[67] T. Hoinka,[72] B. Hokanson-Fasig,[74] K. Hoshina,[74,*] F. Huang,[56] M. Huber,[87] K. Hultqvist,[52] M. Hünnefeld,[72] R. Hussain,[74] S. In,[84] N. Iovine,[50] A. Ishihara,[89] E. Jacobi,[48] G. S. Japaridze,[90] M. Jeong,[84] K. Jero,[74] B. J. P. Jones,[91] P. Kalaczynski,[58] W. Kang,[84] A. Kappes,[76] D. Kappesser,[62] T. Karg,[48] A. Karle,[74] U. Katz,[54] M. Kauer,[74] A. Keivani,[56] J. L. Kelley,[74] A. Kheirandish,[74] J. Kim,[84] T. Kintscher,[48] J. Kiryluk,[92] T. Kittler,[54] S. R. Klein,[71,63] R. Koirala,[81] H. Kolanoski,[83] L. Köpke,[62] C. Kopper,[60] S. Kopper,[93] J. P. Koschinsky,[58] D. J. Koskinen,[51] M. Kowalski,[83,48] K. Krings,[87] M. Kroll,[66] G. Krückl,[62] S. Kunwar,[48] N. Kurahashi,[94] A. Kyriacou,[88] M. Labare,[82] J. L. Lanfranchi,[56] M. J. Larson,[51] F. Lauber,[67] K. Leonard,[74] M. Leuermann,[58] Q. R. Liu,[74] E. Lohfink,[62] C. J. Lozano Mariscal,[76] L. Lu,[89] J. Lünemann,[77] W. Luszczak,[74] J. Madsen,[95] G. Maggi,[77] K. B. M. Mahn,[80] Y. Makino,[89] S. Mancina,[74] R. Maruyama,[96] K. Mase,[89] R. Maunu,[69] K. Meagher,[50] M. Medici,[51] M. Meier,[72] T. Menne,[72] G. Merino,[74] T. Meures,[50] S. Miarecki,[71,63] J. Micallef,[80] G. Momenté,[62] T. Montaruli,[53] R. W. Moore,[60] M. Moulai,[57] R. Nagai,[89] R. Nahnhauer,[48] P. Nakarmi,[93] U. Naumann,[67] G. Neer,[80] H. Niederhausen,[92] S. C. Nowicki,[60] D. R. Nygren,[71] A. Obertacke Pollmann,[67] A. Olivas,[69] A. O'Murchadha,[50] E. O'Sullivan,[52] T. Palczewski,[71,63] H. Pandya,[81] D. V. Pankova,[56] P. Peiffer,[62] J. A. Pepper,[93] C. Pérez de los Heros,[73] D. Pieloth,[72] E. Pinat,[50] A. Pizzuto,[74] M. Plum,[55] P. B. Price,[63] G. T. Przybylski,[71] C. Raab,[50] M. Rameez,[51] L. Rauch,[48] K. Rawlins,[97] I. C. Rea,[87] R. Reimann,[58] B. Relethford,[94] E. Resconi,[87] W. Rhode,[72] M. Richman,[94] S. Robertson,[88] M. Rongen,[58] C. Rott,[84] T. Ruhe,[72] D. Ryckbosch,[82] D. Rysewyk,[80] I. Safa,[74] S. E. Sanchez Herrera,[60] A. Sandrock,[72] J. Sandroos,[62] M. Santander,[93] S. Sarkar,[51,98] S. Sarkar,[60] K. Satalecka,[48] M. Schaufel,[58] P. Schlunder,[72] T. Schmidt,[69] A. Schneider,[74] S. Schöneberg,[66] L. Schumacher,[58] S. Sclafani,[94] D. Seckel,[81] S. Seunarine,[95] J. Soedingrekso,[72] D. Soldin,[81] M. Song,[69] G. M. Spiczak,[95] C. Spiering,[48] J. Stachurska,[48] M. Stamatikos,[64] T. Stanev,[81] A. Stasik,[48] R. Stein,[48] J. Stettner,[58] A. Steuer,[62] T. Stezelberger,[71]

R. G. Stokstad,[71] A. Stössl,[89] N. L. Strotjohann,[48] T. Stuttard,[51] G. W. Sullivan,[69] M. Sutherland,[64] I. Taboada,[79] F. Tenholt,[66] S. Ter-Antonyan,[85] A. Terliuk,[48] S. Tilav,[81] P. A. Toale,[93] M. N. Tobin,[74] C. Tönnis,[84] S. Toscano,[77] D. Tosi,[74] M. Tselengidou,[54] C. F. Tung,[79] A. Turcati,[87] C. F. Turley,[56] B. Ty,[74] E. Unger,[73] M. A. Unland Elorrieta,[76] M. Usner,[48] J. Vandenbroucke,[74] W. Van Driessche,[82] D. van Eijk,[74] N. van Eijndhoven,[77] S. Vanheule,[82] J. van Santen,[48] M. Vraeghe,[82] C. Walck,[52] A. Wallace,[88] M. Wallraff,[58] F. D. Wandler,[60] N. Wandkowsky,[74] T. B. Watson,[91] A. Waza,[58] C. Weaver,[60] M. J. Weiss,[56] C. Wendt,[74] J. Werthebach,[74] S. Westerhoff,[74] B. J. Whelan,[88] N. Whitehorn,[99] K. Wiebe,[62] C. H. Wiebusch,[58] L. Wille,[74] D. R. Williams,[93] L. Wills,[94] M. Wolf,[87] J. Wood,[74] T. R. Wood,[60] E. Woolsey,[60] K. Woschnagg,[63] G. Wrede,[54] D. L. Xu,[74] X. W. Xu,[85] Y. Xu,[92] J. P. Yanez,[60] G. Yodh,[61] S. Yoshida,[89] and T. Yuan[74]

D. Gaggero[100] and D. Grasso[40,41]

[1] *Université de Strasbourg, CNRS, IPHC UMR 7178, F-67000 Strasbourg, France* [b]

[2] *Technical University of Catalonia, Laboratory of Applied Bioacoustics, Rambla Exposició, 08800 Vilanova i la Geltrú, Barcelona, Spain*

[3] *INFN - Sezione di Genova, Via Dodecaneso 33, 16146 Genova, Italy*

[4] *Institut d'Investigació per a la Gestió Integrada de les Zones Costaneres (IGIC) - Universitat Politècnica de València. C/ Paranimf 1, 46730 Gandia, Spain*

[5] *Aix Marseille Univ, CNRS/IN2P3, CPPM, Marseille, France*

[6] *APC, Univ Paris Diderot, CNRS/IN2P3, CEA/Irfu, Obs de Paris, Sorbonne Paris Cité, France*

[7] *IFIC - Instituto de Física Corpuscular (CSIC - Universitat de València) c/ Catedrático José Beltrán, 2 E-46980 Paterna, Valencia, Spain*

[8] *LAM - Laboratoire d'Astrophysique de Marseille, Pôle de l'Étoile Site de Château-Gombert, rue Frédéric Joliot-Curie 38, 13388 Marseille Cedex 13, France*

[9] *National Center for Energy Sciences and Nuclear Techniques, B.P.1382, R. P.10001 Rabat, Morocco*

[10] *INFN - Laboratori Nazionali del Sud (LNS), Via S. Sofia 62, 95123 Catania, Italy*

[11] *Nikhef, Science Park, Amsterdam, The Netherlands*

[12] *Huygens-Kamerlingh Onnes Laboratorium, Universiteit Leiden, The Netherlands*

[13] *University Mohammed V in Rabat, Faculty of Sciences, 4 av. Ibn Battouta, B.P. 1014, R.P. 10000 Rabat, Morocco*

[14] *Institute of Space Science, RO-077125 Bucharest, Măgurele, Romania*

[15] *Universiteit van Amsterdam, Instituut voor Hoge-Energie Fysica, Science Park 05, 1098 XG Amsterdam, The Netherlands*

[16] *INFN - Sezione di Roma, P.le Aldo Moro 2, 00185 Roma, Italy*

[17] *Dipartimento di Fisica dell'Università La Sapienza, P.le Aldo Moro 2, 00185 Roma, Italy*

[18] *Gran Sasso Science Institude, Viale Francesco Crispi 7, I-00167 L'Aquila, Italy*

[19] *LPHEA, Faculty of Science - Semlali, Cadi Ayyad University, P.O.B. 2390, Marrakech, Morocco.*

[20] *INFN - Sezione di Bologna, Viale Berti-Pichat 6/2, 40127 Bologna, Italy*

[21] *INFN - Sezione di Bari, Via E. Orabona 4, 70126 Bari, Italy*

[22] *Department of Computer Architecture and Technology/CITIC, University of Granada, 18071 Granada, Spain*

[23] *Géoazur, UCA, CNRS, IRD, Observatoire de la Côte d'Azur, Sophia Antipolis, France*

[24] *Dipartimento di Fisica dell'Università, Via Dodecaneso 33, 16146 Genova, Italy*

[25] *Université Paris-Sud, 91405 Orsay Cedex, France*

[26] *Université de Strasbourg, CNRS, IPHC UMR 7178, F-67000 Strasbourg, France*

[27] *Friedrich-Alexander-Universität Erlangen-Nürnberg, Erlangen Centre for Astroparticle Physics, Erwin-Rommel-Str. 1, 91058 Erlangen, Germany*

[28] *University Mohammed I, Laboratory of Physics of Matter and Radiations, B.P.717, Oujda 6000, Morocco*

[29] *Institut für Theoretische Physik und Astrophysik, Universität Würzburg, Emil-Fischer Str. 31, 97074 Würzburg, Germany*

[30] *Dipartimento di Fisica e Astronomia dell'Università, Viale Berti Pichat 6/2, 40127 Bologna, Italy*

[31] *Laboratoire de Physique Corpusculaire, Clermont Université, Université Blaise Pascal, CNRS/IN2P3, BP 10448, F-63000 Clermont-Ferrand, France*

[32] *LIS, UMR Université de Toulon, Aix Marseille Université, CNRS, 83041 Toulon, France*

[33] *Royal Netherlands Institute for Sea Research (NIOZ) and Utrecht University, Landsdiep 4, 1797 SZ 't Horntje (Texel), the Netherlands*

[34] *Institut Universitaire de France, 75005 Paris, France*

[35] *Dr. Remeis-Sternwarte and ECAP, Friedrich-Alexander-Universität Erlangen-Nürnberg, Sternwartstr. 7, 96049 Bamberg, Germany*

[36] *Moscow State University, Skobeltsyn Institute of Nuclear Physics, Leninskie gory, 119991 Moscow, Russia*

[37] *Mediterranean Institute of Oceanography (MIO), Aix-Marseille University, 13288, Marseille, Cedex 9, France; Université du Sud Toulon-Var, CNRS-INSU/IRD UM 110, 83957, La Garde Cedex, France*

[38] *INFN - Laboratori Nazionali del Sud (LNS), Via S. Sofia 64, 95123 Catania, Italy*

[b] antares.spokesperson@in2p3.fr

[39] *Direction des Sciences de la Matière - Institut de recherche sur les lois fondamentales de l'Univers - Service de Physique des Particules, CEA Saclay, 91191 Gif-sur-Yvette Cedex, France*
[40] *INFN - Sezione di Pisa, Largo B. Pontecorvo 3, 56127 Pisa, Italy*
[41] *Dipartimento di Fisica dell'Università, Largo B. Pontecorvo 3, 56127 Pisa, Italy*
[42] *INFN - Sezione di Napoli, Via Cintia 80126 Napoli, Italy*
[43] *Dipartimento di Fisica dell'Università Federico II di Napoli, Via Cintia 80126, Napoli, Italy*
[44] *Universiteit van Amsterdam, Instituut voor Hoge-Energie Fysica, Science Park 105, 1098 XG Amsterdam, The Netherlands*
[45] *Dpto. de Física Teórica y del Cosmos & C.A.F.P.E., University of Granada, 18071 Granada, Spain*
[46] *GRPHE - Université de Haute Alsace - Institut universitaire de technologie de Colmar, 34 rue du Grillenbreit BP 50568 - 68008 Colmar, France*
[47] *Dept. of Physics and Astronomy, University of Canterbury, Private Bag 4800, Christchurch, New Zealand* [c]
[48] *DESY, D-15738 Zeuthen, Germany*
[49] *Dept. of Physics and Astronomy, University of Canterbury, Private Bag 4800, Christchurch, New Zealand*
[50] *Université Libre de Bruxelles, Science Faculty CP230, B-1050 Brussels, Belgium*
[51] *Niels Bohr Institute, University of Copenhagen, DK-2100 Copenhagen, Denmark*
[52] *Oskar Klein Centre and Dept. of Physics, Stockholm University, SE-10691 Stockholm, Sweden*
[53] *Département de physique nucléaire et corpusculaire, Université de Genève, CH-1211 Genève, Switzerland*
[54] *Erlangen Centre for Astroparticle Physics, Friedrich-Alexander-Universität Erlangen-Nürnberg, D-91058 Erlangen, Germany*
[55] *Department of Physics, Marquette University, Milwaukee, WI, 53201, USA*
[56] *Dept. of Physics, Pennsylvania State University, University Park, PA 16802, USA*
[57] *Dept. of Physics, Massachusetts Institute of Technology, Cambridge, MA 02139, USA*
[58] *III. Physikalisches Institut, RWTH Aachen University, D-52056 Aachen, Germany*
[59] *Physics Department, South Dakota School of Mines and Technology, Rapid City, SD 57701, USA*
[60] *Dept. of Physics, University of Alberta, Edmonton, Alberta, Canada T6G 2E1*
[61] *Dept. of Physics and Astronomy, University of California, Irvine, CA 92697, USA*
[62] *Institute of Physics, University of Mainz, Staudinger Weg 7, D-55099 Mainz, Germany*
[63] *Dept. of Physics, University of California, Berkeley, CA 94720, USA*
[64] *Dept. of Physics and Center for Cosmology and Astro-Particle Physics, Ohio State University, Columbus, OH 43210, USA*
[65] *Dept. of Astronomy, Ohio State University, Columbus, OH 43210, USA*
[66] *Fakultät für Physik & Astronomie, Ruhr-Universität Bochum, D-44780 Bochum, Germany*
[67] *Dept. of Physics, University of Wuppertal, D-42119 Wuppertal, Germany*
[68] *Dept. of Physics and Astronomy, University of Rochester, Rochester, NY 14627, USA*
[69] *Dept. of Physics, University of Maryland, College Park, MD 20742, USA*
[70] *Dept. of Physics and Astronomy, University of Kansas, Lawrence, KS 66045, USA*
[71] *Lawrence Berkeley National Laboratory, Berkeley, CA 94720, USA*
[72] *Dept. of Physics, TU Dortmund University, D-44221 Dortmund, Germany*
[73] *Dept. of Physics and Astronomy, Uppsala University, Box 516, S-75120 Uppsala, Sweden*
[74] *Dept. of Physics and Wisconsin IceCube Particle Astrophysics Center, University of Wisconsin, Madison, WI 53706, USA*
[75] *SNOLAB, 1039 Regional Road 24, Creighton Mine 9, Lively, ON, Canada P3Y 1N2*
[76] *Institut für Kernphysik, Westfälische Wilhelms-Universität Münster, D-48149 Münster, Germany*
[77] *Vrije Universiteit Brussel (VUB), Dienst ELEM, B-1050 Brussels, Belgium*
[78] *Dept. of Astronomy and Astrophysics, Pennsylvania State University, University Park, PA 16802, USA*
[79] *School of Physics and Center for Relativistic Astrophysics, Georgia Institute of Technology, Atlanta, GA 30332, USA*
[80] *Dept. of Physics and Astronomy, Michigan State University, East Lansing, MI 48824, USA*
[81] *Bartol Research Institute and Dept. of Physics and Astronomy, University of Delaware, Newark, DE 19716, USA*
[82] *Dept. of Physics and Astronomy, University of Gent, B-9000 Gent, Belgium*
[83] *Institut für Physik, Humboldt-Universität zu Berlin, D-12489 Berlin, Germany*
[84] *Dept. of Physics, Sungkyunkwan University, Suwon 440-746, Korea*
[85] *Dept. of Physics, Southern University, Baton Rouge, LA 70813, USA*
[86] *Dept. of Astronomy, University of Wisconsin, Madison, WI 53706, USA*
[87] *Physik-department, Technische Universität München, D-85748 Garching, Germany*
[88] *Department of Physics, University of Adelaide, Adelaide, 5005, Australia*
[89] *Dept. of Physics and Institute for Global Prominent Research, Chiba University, Chiba 263-8522, Japan*
[90] *CTSPS, Clark-Atlanta University, Atlanta, GA 30314, USA*

[c] analysis@icecube.wisc.edu

[91] Dept. of Physics, University of Texas at Arlington, 502 Yates St., Science Hall Rm 108, Box 19059, Arlington, TX 76019, USA
[92] Dept. of Physics and Astronomy, Stony Brook University, Stony Brook, NY 11794-3800, USA
[93] Dept. of Physics and Astronomy, University of Alabama, Tuscaloosa, AL 35487, USA
[94] Dept. of Physics, Drexel University, 3141 Chestnut Street, Philadelphia, PA 19104, USA
[95] Dept. of Physics, University of Wisconsin, River Falls, WI 54022, USA
[96] Dept. of Physics, Yale University, New Haven, CT 06520, USA
[97] Dept. of Physics and Astronomy, University of Alaska Anchorage, 3211 Providence Dr., Anchorage, AK 99508, USA
[98] Dept. of Physics, University of Oxford, 1 Keble Road, Oxford OX1 3NP, UK
[99] Department of Physics and Astronomy, UCLA, Los Angeles, CA 90095, USA
[100] GRAPPA, University of Amsterdam, Science Park 904, 1098 XH Amsterdam, Netherlands

Submitted to ApJL

ABSTRACT

The existence of diffuse Galactic neutrino production is expected from cosmic ray interactions with Galactic gas and radiation fields. Thus, neutrinos are a unique messenger offering the opportunity to test the products of Galactic cosmic ray interactions up to energies of hundreds of TeV. Here we present a search for this production using ten years of ANTARES track and shower data, as well as seven years of IceCube track data. The data are combined into a joint likelihood test for neutrino emission according to the KRA_γ model assuming a 5 PeV per nucleon Galactic cosmic ray cutoff. No significant excess is found. As a consequence, the limits presented in this work start constraining the model parameter space for Galactic cosmic ray production and transport.

Keywords: neutrinos — cosmic rays — diffusion — Galaxy: disk — gamma rays: diffuse background

1. INTRODUCTION

A diffuse Galactic neutrino emission is expected from cosmic ray (CR) interactions with interstellar gas and radiation fields. These interactions are also the dominant production mechanism of the diffuse high-energy γ-rays in the Galactic plane, which have been measured by the *Fermi*-Large Area Telescope (*Fermi*-LAT) (Ackermann et al. 2012).

In the GALPROP-based (Vladimirov et al. 2011) conventional model of Galactic diffuse γ-ray production CRs are accelerated in a distribution of sources such as supernova remnants. They propagate diffusively in the interstellar medium producing γ-rays and neutrinos via interactions with the interstellar radiation field and interstellar gas. The interstellar radiation field is weakly constrained by *Fermi*-LAT γ-ray data and interstellar gas is constrained by both *Fermi*-LAT γ-ray data and radio measurements of CO and HI line intensities. The CR population model itself is normalised to local measurements taken at Earth. The GALPROP model parameters are tuned to achieve optimal agreement between *Fermi*-LAT (Ackermann et al. 2012) data and the direction-dependent prediction given by integrating expected γ-ray yields along the line of sight from Earth. The neutral pion decay component estimated by the conventional model should be accompanied by a neutrino flux from charged pion decay.

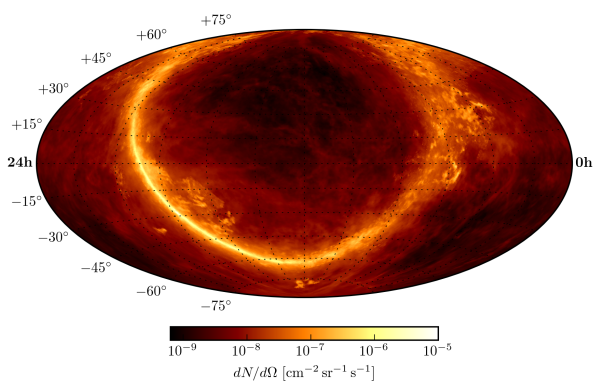

Figure 1. Neutrino flux per unit of solid angle of the KRA_γ^5 model (Gaggero et al. 2015a), shown as a function of direction in equatorial coordinates (Hammer projection).

The conventional model, however, under-predicts the γ-ray flux above 10 GeV in the inner Galaxy (Ackermann et al. 2012). The KRA_γ models (Gaggero et al. 2015a,b, 2017) address this issue using a radially-dependent model for the CR diffusion coefficient and the advective wind. The primary CR spectrum assumed within the KRA_γ models has an exponential cutoff at

* Earthquake Research Institute, University of Tokyo, Bunkyo, Tokyo 113-0032, Japan

a certain energy. In order to bracket measurements by KASCADE (Antoni et al. 2005) and KASCADE-Grande (Apel et al. 2013), respectively in the [100 TeV, 100 PeV] and [10 PeV, 2000 PeV] energy ranges, while maintaining agreement with proton and helium measurements by CREAM (Ahn et al. 2010), cutoffs at 5 and 50 PeV per nucleon are considered. The resulting models are referred to as KRA_γ^5 and KRA_γ^{50}, respectively. The direction dependence of the energy-integrated KRA_γ^5 neutrino flux prediction is shown in Figure 1. Compared to the conventional model of the Galactic diffuse emission, the KRA_γ models predict modified spectra and enhanced overall γ-ray and neutrino fluxes in the southern sky, especially in the central ridge where a hardening of the CR spectra is reproduced. Hence, neutrinos offer a unique opportunity to independently test the model assumptions of Galactic CR production and transport, accessing energies far beyond the reach of current γ-ray experiments.

The KRA_γ predictions have already been tested separately with ANTARES (Albert et al. 2017) and IceCube (Aartsen et al. 2017a) data. ANTARES and IceCube achieved sensitivities of $1.05 \times \Phi_{\mathrm{KRA}_\gamma^{50}}$ and $0.79 \times \Phi_{\mathrm{KRA}_\gamma^{50}}$, respectively; both analyses obtained 90% confidence level (CL) upper limits of $1.2 \times \Phi_{\mathrm{KRA}_\gamma^{50}}$. ANTARES additionally examined the 5 PeV cutoff model, obtaining a sensitivity of $1.4 \times \Phi_{\mathrm{KRA}_\gamma^5}$ and an upper limit of $1.1 \times \Phi_{\mathrm{KRA}_\gamma^5}$ due to an under-fluctuation of the fitted signal flux in the track channel.

This paper presents a combination of these two maximum-likelihood analyses exploiting the advantageous field of view of ANTARES as well as the high statistics of IceCube.

2. DETECTORS AND DATA SAMPLES

The IceCube Neutrino Observatory (Aartsen et al. 2017b) is located at the South Pole between 1.45 and 2.45 km below the surface of the ice. It consists of 5160 photomultiplier tubes (PMTs) instrumenting one cubic kilometer of ice. The ANTARES neutrino telescope (Ageron et al. 2011) consists of 885 PMTs deployed in the Mediterranean sea, 40 km off the coast of Toulon, France. It is installed at depths between 2.01 km and 2.47 km below sea level, instrumenting a volume of $\sim$0.01 km^3.

Neutrinos interacting with matter produce charged particles that generate Cherenkov light in the detectors. From the collected Cherenkov light, the energy and direction of the incoming neutrinos are reconstructed. A muon neutrino[1] undergoing a charged current interaction produces a muon that can travel large distances through the medium, leading to a *track* event topology in the detector. Most other interactions produce a nearly spherical *shower* event topology. In this analysis, ANTARES events of both topologies are used, while only track events are taken from IceCube data.

The ANTARES event sample used in this work includes the one used in (Albert et al. 2017) extended by the data collected in 2016. These data use the most recent offline-reconstructed dataset, incorporating dedicated calibrations of positioning, timing and efficiency (Adrián-Martínez et al. 2012). The sample is taken from a total of 2780 days of detector livetime, over a total of ten calendar years. Part of the sample was collected with partially-completed detector configurations. Here, 218 shower(-like) events are selected, while 2.6 signal events are expected from the KRA_γ^5 model. For these signal events we have a median angular resolution of 2.4°. The track selection includes 7,850 events, with 10.2 signal events expected having an angular resolution of 0.5°. The energy ranges including 90% of signal events are [2.1 TeV, 150 TeV] for showers and [360 GeV, 130 TeV] for tracks.

The IceCube seven-year track selection used in this analysis is detailed by Aartsen et al. (2017c). It results in a total of 730,130 events with 191 events expected from the KRA_γ^5 model. The dataset was collected over a total of 2431 days of detector livetime, some of which took place during the construction phase of the detector. The IceCube signal events are expected to have median angular resolution of 0.8°. The energy range containing 90% of the expected signal events is [390 GeV, 110 TeV].

The energy range in which the combined analysis is valid is [90 GeV, 300 TeV]. This range is defined as containing 90% of the sensitivity. It is calculated by finding the low and high energy thresholds where removing simulated signal events outside these values worsens the sensitivity by 5% each.

3. SEARCH METHOD

The present analysis uses an unbinned likelihood ratio test. The likelihood functions for each sample — ANTARES tracks, ANTARES showers, and IceCube tracks — are defined as

$$\mathcal{L}_{\mathrm{sig+bkg}}(n_{\mathrm{sig}}) = \prod_i \Big[\frac{n_{\mathrm{sig}}}{N} \cdot \mathcal{S}(E_i, \alpha_i, \delta_i) + (1 - \frac{n_{\mathrm{sig}}}{N}) \cdot \mathcal{B}(E_i, \delta_i) \Big] , \quad (1)$$

[1] In the following, particles also refer to the corresponding antiparticles.

where N is the total number of events; $n_{\rm sig}$ is the number of signal events; $\mathcal{S}$ is the signal probability density function (PDF) for an event i at the equatorial coordinates (α_i, δ_i) with energy E_i. It is obtained from Monte Carlo simulations of the detectors with the model flux as input - it is proportional to the expected signal rate at a given reconstructed energy and direction. $\mathcal{B}$ is the PDF of the background.

Minor differences in the original, separate ANTARES and IceCube PDF constructions are preserved in this work. For IceCube tracks, the background term $\mathcal{B}$ comes from the data with a correction for the signal contamination expected for $n_{\rm sig}$ signal events (Aartsen et al. 2017a). For the ANTARES samples, this is approximated by ignoring the signal correction term (Albert et al. 2017). In addition, the IceCube signal PDF accounts for the estimated point spread function of each event, while average point spread functions are used for track and shower ANTARES events.

In order to account for the different acceptances of each sample as well as any bias in the fitted signal normalization, we forward-fold the signal flux $\Phi_{\rm sig}$ into the individual likelihoods using a response function obtained from simulated pseudo-experiments.

Then the combined likelihood is simply the product over the per-sample likelihoods. The combined test statistic is the log-likelihood ratio evaluated for that $\Phi_{\rm sig}$ which maximizes the combined likelihood:

$$\mathrm{TS}_{\rm comb} = \max_{\Phi_{\rm sig}} \left\{ \sum_{\rm sample} \ln \left[\frac{\mathcal{L}_{\rm sig+bkg}(\Phi_{\rm sig})}{\mathcal{L}_{\rm bkg}} \right] \right\}, \qquad (2)$$

where $\mathrm{TS}_{\rm comb}$ is the combined test statistic, $\mathcal{L}_{\rm bkg} = \mathcal{L}_{\rm sig+bkg}(\Phi_{\rm sig} = 0)$ is the likelihood to have only background and the sum runs over the event samples. This is illustrated in Figure 2 with the combined log-likelihood ratio and $\mathrm{TS}_{\rm comb}$ fit for the KRA^5_γ model.

The combined and independent sensitivities are summarized in Table 1. They are defined as the median upper limit[2]. The combination is not only a way to exploit more data with different systematics but also an opportunity to benefit from the complementarity of the two detectors. While IceCube has much higher statistics than ANTARES, we show in Figure 3 (a) that ANTARES offers enhanced sensitivity in the southern sky where a larger flux is expected. This favorable view is coupled with relatively better angular resolution for ANTARES than IceCube. In Figure 3 (b) we show that while IceCube can in principle detect higher energy events compared to ANTARES, the direction-dependent model spectra studied here result in similar energy ranges being tested by both detectors. Overall, the relative contribution of IceCube to the sensitivity is 61%; for ANTARES tracks and showers the relative contributions are 25% and 14%, respectively.

[2] It is defined as the average upper limit in the ANTARES only analysis (Albert et al. 2017). This and the addition of 2016 data account for the difference in the ANTARES sensitivities.

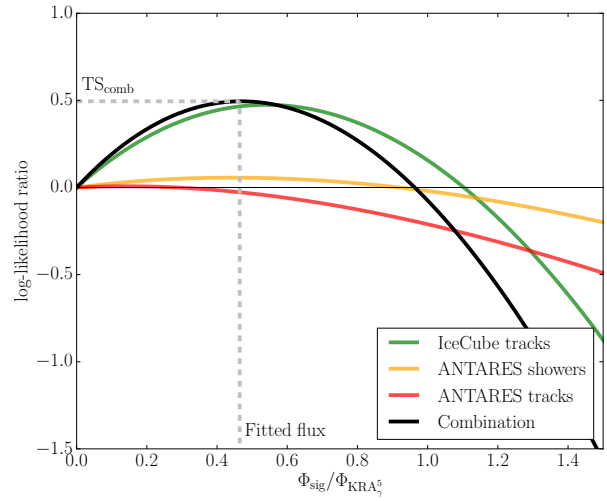

Figure 2. Combination of the log-likelihood ratio curves and fitting of the flux on the combined test statistic. These curves correspond to the unblinded data using the likelihood for the KRA^5_γ model.

4. RESULTS AND DISCUSSION

This analysis combines seven years of IceCube tracks and ten years of ANTARES tracks and showers using a likelihood ratio test. The results are summarized in Table 1. Systematic uncertainties on the ANTARES detection efficiency (due to the uncertainty on the acceptance of the ANTARES PMTs) are included in the analysis as in the paper by Albert et al. (2017). As described by Aartsen et al. (2017c), systematic uncertainties in the modeling of the Antarctic ice and the optical module efficiency lead to an uncertainty on the IceCube detection efficiency of at most 11% which is not included here.

The maximum-likelihood estimate yields a non-zero diffuse Galactic neutrino flux for both models with a p-value of 29% for KRA^5_γ and 26% for KRA^{50}_γ. Since neither of these results is statistically significant, we place upper-limits on both model normalizations. The KRA^{50}_γ model is constrained at the 90% confidence level (with an upper limit of $0.9 \times \Phi_{\mathrm{KRA}^{50}_\gamma}$), while the KRA^5_γ model is not yet constrained by our analysis. This was expected as the 50 PeV cutoff represents an extreme tuning of the acceleration parameters for the Galactic CRs, while the

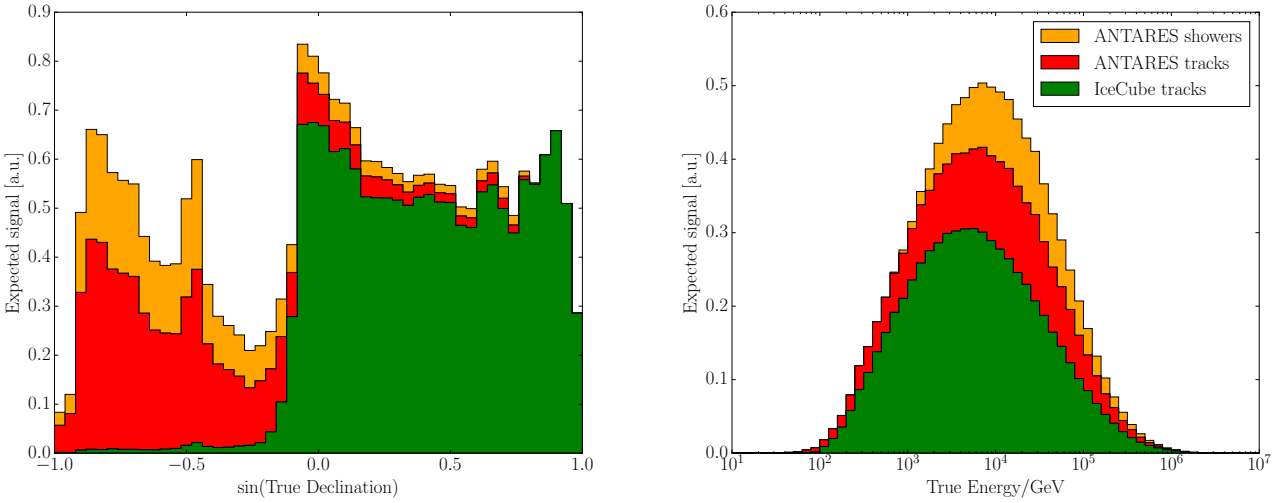

(a) (b)

Figure 3. Stacked histograms (i.e., every bin shows the fractional contribution of every sample summed on top of each other) of the signal expected from the KRA_γ^5 model as function of the declination (a) and energy (b) Monte Carlo truth. The colored area of each histogram represents the relative contribution to the sensitivity of this event sample. The relative contribution to the sensitivity is defined as the difference in the sensitivity flux resulting from the addition of a certain event sample divided by the combined sensitivity flux.

Table 1. Sensitivities and results of the analysis on the KRA_γ models with the 5 and 50 PeV cutoffs.

Energy cutoff	Sensitivity $[\Phi_{\mathrm{KRA}_\gamma}]$			Fitted flux	p-value	UL at 90% CL
	Combined	ANTARES	IceCube	$[\Phi_{\mathrm{KRA}_\gamma}]$	[%]	$[\Phi_{\mathrm{KRA}_\gamma}]$
5 PeV	0.81	1.21	1.14	0.47	29	1.19
50 PeV	0.57	0.94	0.82	0.37	26	0.90

5 PeV cutoff in light CR can be considered a more reliable case for the Galactic accelerators.

Figure 4 represents the combined upper limits in comparison to the all-flavor full sky energy spectrum of the KRA_γ models as well as the previous IceCube and ANTARES upper limits. The present upper limit on the 5 PeV model is higher than the previously published upper limit for ANTARES alone although the sensitivity is much better. This is due to the overfluctuation observed in the IceCube data sample as well as the difference in the definition of the test statistic. In the ANTARES standalone analysis it was the sum of the shower and track test statistics, computed independently, instead of computing one test statistic from the combined log-likelihood ratio curve (equation 2).

The results presented here provide for the first time a combined constraint on diffuse Galactic neutrino emission by IceCube and ANTARES. The limit on the KRA_γ model with 50 PeV cutoff extends the energy range of the constraint on the model from 10 GeV with *Fermi*-LAT up to hundreds of TeV. Based on the limit on the KRA_γ^5-model, this analysis limits the total flux contribution of diffuse Galactic neutrino emission to the total astrophysical signal reported by Aartsen et al. (2015) to 8.5%. In the future, the sensitivity of this analysis can be further improved by including IceCube showers (Aartsen et al. 2017d). This will allow for a powerful test of the KRA_γ^5 model, thereby constraining the diffusion mechanisms, the maximal energy injected by supernova remnants and the Galactic gas distributions considered in the model.

ANTARES acknowledges the financial support of the funding agencies: Centre National de la Recherche Scientifique (CNRS), Commissariat à l'énergie atomique et aux énergies alternatives (CEA), Commission Européenne (FEDER fund and Marie Curie Program), Institut Universitaire de France (IUF), IdEx program and UnivEarthS Labex program at Sorbonne Paris Cité (ANR-10-LABX-0023 and ANR-11-IDEX-0005-02), Labex OCEVU (ANR-11-LABX-0060) and the A*MIDEX project (ANR-11-IDEX-0001-02), Région

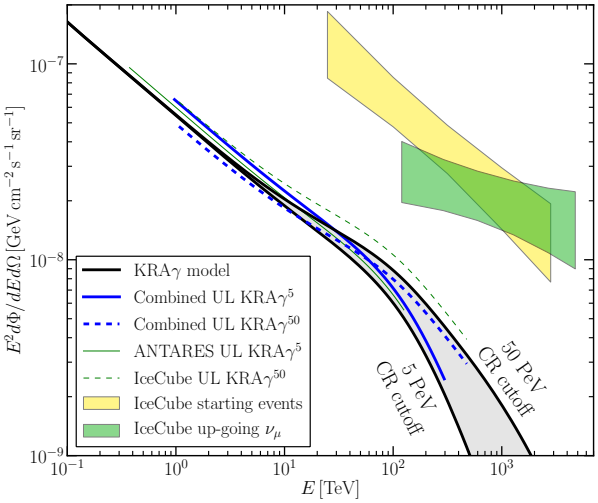

Figure 4. Combined upper limits (UL) at 90% confidence level (blue lines) on the three-flavor neutrino flux of the KRA$_\gamma$ model with the 5 and 50 PeV cutoffs (black lines). The boxes represent the diffuse astrophysical neutrino fluxes measured by IceCube using an isotropic flux template with starting events (yellow) and upgoing tracks (green).

Île-de-France (DIM-ACAV), Région Alsace (contrat CPER), Région Provence-Alpes-Côte d'Azur, Département du Var and Ville de La Seyne-sur-Mer, France; Bundesministerium für Bildung und Forschung (BMBF), Germany; Istituto Nazionale di Fisica Nucleare (INFN), Italy; Nederlandse organisatie voor Wetenschappelijk Onderzoek (NWO), the Netherlands; Council of the President of the Russian Federation for young scientists and leading scientific schools supporting grants, Russia; National Authority for Scientific Research (ANCS), Romania; Ministerio de Economía y Competitividad (MINECO): Plan Estatal de Investigación (refs. FPA2015-65150-C3-1-P, -2-P and -3-P, (MINECO/FEDER)), Severo Ochoa Centre of Excellence and MultiDark Consolider (MINECO), and Prometeo and Grisolía programs (Generalitat Valenciana), Spain; Ministry of Higher Education, Scientific Research and Professional Training, Morocco. We also acknowledge the technical support of Ifremer, AIM and Foselev Marine for the sea operation and the CC-IN2P3 for the computing facilities.

The IceCube Neutrino Observatory acknowledges support from the following agencies: USA – U.S. National Science Foundation-Office of Polar Programs, U.S. National Science Foundation-Physics Division, Wisconsin Alumni Research Foundation, Center for High Throughput Computing (CHTC) at the University of Wisconsin-Madison, Open Science Grid (OSG), Extreme Science and Engineering Discovery Environment (XSEDE), U.S. Department of Energy-National Energy Research Scientific Computing Center, Particle astrophysics research computing center at the University of Maryland, Institute for Cyber-Enabled Research at Michigan State University, and Astroparticle physics computational facility at Marquette University; Belgium – Funds for Scientific Research (FRS-FNRS and FWO), FWO Odysseus and Big Science programmes, and Belgian Federal Science Policy Office (Belspo); Germany – Bundesministerium für Bildung und Forschung (BMBF), Deutsche Forschungsgemeinschaft (DFG), Helmholtz Alliance for Astroparticle Physics (HAP), Initiative and Networking Fund of the Helmholtz Association, Deutsches Elektronen Synchrotron (DESY), and High Performance Computing cluster of the RWTH Aachen; Sweden – Swedish Research Council, Swedish Polar Research Secretariat, Swedish National Infrastructure for Computing (SNIC), and Knut and Alice Wallenberg Foundation; Australia – Australian Research Council; Canada – Natural Sciences and Engineering Research Council of Canada, Calcul Québec, Compute Ontario, Canada Foundation for Innovation, WestGrid, and Compute Canada; Denmark – Villum Fonden, Danish National Research Foundation (DNRF); New Zealand – Marsden Fund; Japan – Japan Society for Promotion of Science (JSPS) and Institute for Global Prominent Research (IGPR) of Chiba University; Korea – National Research Foundation of Korea (NRF); Switzerland – Swiss National Science Foundation (SNSF).

The IceCube Collaboration designed, constructed and now operates the IceCube Neutrino Observatory. Data processing and calibration, Monte Carlo simulations of the detector and of theoretical models, and data analyses were performed by a large number of collaboration members, who also discussed and approved the scientific results presented here. It was reviewed by the entire collaboration before publication, and all authors approved the final version of the manuscript.

The main authors of this manuscript were Jon Dumm, Timothée Grégoire, Christian Haack and Michael Richman.

REFERENCES

Aartsen, M. G., Abraham, K., Ackermann, M., et al. 2015, ApJ, 809, 98

Aartsen, M. G., Ackermann, M., Adams, J., et al. 2017a, ApJ, 849, 67

—. 2017b, Journal of Instrumentation, 12, P03012

Aartsen, M. G., Abraham, K., Ackermann, M., et al. 2017c, ApJ, 835, 151

Aartsen, M. G., et al. 2017d, ApJ, 846, 136

Ackermann, M., Ajello, M., Atwood, W. B., et al. 2012, ApJ, 750, 3

Adrián-Martínez, S., Ageron, M., Aguilar, J. A., et al. 2012, Journal of Instrumentation, 7, T08002

Ageron, M., Aguilar, J. A., Al Samarai, I., et al. 2011, Nucl. Instrum. Meth., A656, 11

Ahn, H. S., Allison, P., Bagliesi, M. G., et al. 2010, ApJ, 714, L89

Albert, A., André, M., Anghinolfi, M., et al. 2017, PhRvD, 96, 062001

Antoni, T., Apel, W. D., Badea, A. F., et al. 2005, Astropart. Phys., 24, 1

Apel, W. D., Arteaga-Velàzquez, J. C., Bekk, K., et al. 2013, Astropart. Phys., 47, 54

Gaggero, D., Grasso, D., Marinelli, A., Taoso, M., & Urbano, A. 2017, PhRvL, 119, 031101

Gaggero, D., Grasso, D., Marinelli, A., Urbano, A., & Valli, M. 2015a, ApJ, 815, L25

Gaggero, D., Urbano, A., Valli, M., & Ullio, P. 2015b, PhRvD, D91, 083012

Vladimirov, A. E., Digel, S. W., Jóhannesson, G., et al. 2011, Computer Physics Communications, 182, 1156